

第二结构导向剂诱导形成的二维有机模板稀土硫酸盐

石 杰¹ 成伟唯² 郑 磊¹ 许 岩^{*1}

(¹ 南京工业大学化工学院, 材料化学工程国家重点实验室, 南京 210009)

(² 南京师范大学泰州学院化学与生物工程学院, 泰州 225300)

摘要: 水热条件下合成了具有超大孔道和层状结构的有机模板稀土硫酸盐。超大孔道的稀土硫酸盐(**1**)的分子式为 $[(\text{CH}_3)_2\text{NH}_2]_9[\text{Pr}_5(\text{SO}_4)_{12}] \cdot 2\text{H}_2\text{O}$, 它展现出有趣的交叉二十元环孔道结构。层状的稀土硫酸盐的分子式为 $[\text{H}_3\text{O}]_3[(\text{CH}_3)_2\text{NH}_2]_3[\text{Ln}_2(\text{SO}_4)_6]$ ($\text{Ln}=\text{Pr}$, **2**; Nd , **3**), 它可以被看作是由双链和八元环结合而成。这 3 种化合物的合成揭示了大的有机胺(三聚氰胺)可能用作第二结构导向剂, 阻止形成高维数的无机骨架, 从而诱导了二维层状结构稀土硫酸盐晶体的生长。对化合物 **1** 和 **3** 的磁性进行了研究, 测试的温度范围在 2~300 K。

关键词: 稀土硫酸盐; 二十元环孔道; 结构导向剂; 磁性

中图分类号: O614.33+4; O614.33+5

文献标识码: A

文章编号: 1001-4861(2017)11-2083-12

DOI: 10.11862/CJIC.2017.253

Formation of 2D Organic Templated Lanthanide Sulfates Induced by Second Structural Directing Agent

SHI Jie¹ CHENG Wei-Wei² ZHENG Lei¹ XU Yan^{*1}

(¹ College of Chemistry and Chemical Engineering, State Key Laboratory of Materials-Oriented
Chemical Engineering, Nanjing Tech University, Nanjing 210009, China)

(² School of Chemistry and Bioengineering, Nanjing Normal University Taizhou College, Taizhou, Jiangsu 225300, China)

Abstract: Extra-large-pore and layered organically templated lanthanide sulfates have been prepared under solvothermal conditions. The extra-large-pore lanthanide sulfates, with the composition $[(\text{CH}_3)_2\text{NH}_2]_9[\text{Pr}_5(\text{SO}_4)_{12}] \cdot 2\text{H}_2\text{O}$ (**1**), exhibit an interestingly intersecting 20-membered ring channels. The layered lanthanide sulfates, formulated as $[\text{H}_3\text{O}]_3[(\text{CH}_3)_2\text{NH}_2]_3[\text{Ln}_2(\text{SO}_4)_6]$ ($\text{Ln}=\text{Pr}$ for **2**, Nd for **3**), can be considered as combination of double-stranded chains and 8-membered rings. The synthesis of three compounds demonstrates that large organic amine (1,3,5-triazine-2,4,6-triamine) may be used as the second structural directing agent to prevent the formation of high dimensional inorganic framework as well as inducing crystal the growth of 2D layer structural lanthanide sulfates. The magnetic property of compounds **1** and **3** has been investigated through the magnetic measurement over the temperature range of 2~300 K. CCDC: 1553358, **1**; 1553359, **2**; 1553360, **3**.

Keywords: lanthanide sulfates; 20-membered ring channels; structural directing agent; magnetic property

收稿日期: 2017-06-01。收修改稿日期: 2017-09-11。

国家自然科学基金(No.21571103)资助项目。

*通信联系人。E-mail: yanxu@njtech.edu.cn

0 Introduction

Tremendous progress have been made to synthesize new porous materials with pure tetrahedral or mixed polyhedral open-frameworks, while studies of new topological microporous structures of extra-large-pore (more than 12 membered ring channels) open frameworks are extremely intensive because of the widespread applications of these materials in catalysis, ion exchanging, magnetic properties and the separation of large molecules such as heavy oils or pharmaceuticals^[1]. Since the discovery of the first molecular sieve containing extra-large 18-membered rings (18MR), aluminophosphate VPI-5^[2], many metal phosphates, aluminosilicates and germanates with extra-large-pore open frameworks have been synthesized^[3]. A few open-framework structures with extra-large 16-ring channels have been described (Table 1). Recently, studies focusing on the organic templated lanthanide sulfates have been an important advancement in the field of solid state materials^[4-6]. Compared with Ge, Zn and Al, the rare-earth elements can adopt a large range of coordination numbers from 8 to 12 and flexible Ln-O bond lengths^[7-9]. The S-O bonds have less charge (0.5) than the P-O bonds (0.75), which could create difficulties in forming extended network structures^[14]. The high coordination number offers the possibility to generate open-frameworks with high

charge densities, which may result in novel topological structures with large pores^[10]. Unfortunately, to date, extra-large-pore structures of lanthanide sulfates only have a few successful examples. Our group has been reported two extra-large-pore structures of europium and terbium sulfates^[8,12]. As a part of our previous work, we also have been synthesized two more extra-large-pore structures of lanthanide sulfates. Recently, we reported that in the presence of large organic amines, lanthanide elements can be easily coordinated by water to form 1D or 2D architectures^[8]. Herein, we reported another extra-large-pore structures of lanthanide sulfates and two 2D layered lanthanide sulfates containing double-stranded chains by using a small amine, *viz.*, dimethylamine as a structural directing agent (SDA) and a large amine, *viz.*, 1,3,5-triazine-2,4,6-triamine as a second SDA.

More recently, other topics in the solid state materials chemistry are the inorganic materials with double-stranded chains due to their particularly desirable applications in optical materials and enantiotopic selective separation. But there is only a few metal sulfates containing this double-stranded chain^[11]. For example, $[\text{H}_3\text{N}(\text{CH}_2)_2\text{NH}_3][\text{FeF}_3(\text{SO}_4)]$ ^[11a] contains double-stranded chain. In our previous work, we reported that 1,3,5-triazine-2,4,6-triamine as a second SDA induce the formation of 1D organic templated terbium sulfate^[12]. Herein, second SDA

Table 1 Examples for open framework materials with 16MR channels

Material	Formula	Max. pore dimension	Ref.
	$[\text{Zn}_3(\text{O}_3\text{PCH}_2\text{CO}_2)_2(\text{O}_3\text{PCH}_2\text{CO}_2\text{H})][(\text{C}_2\text{N}_2\text{H}_{10})(\text{btc})]$	24	[3a]
ZnHPO-CJ2	$(\text{C}_6\text{H}_{14}\text{N})_2[\text{Zn}_3(\text{HPO}_3)_4]$	24	[3b]
NTHU-5	$(\text{C}_4\text{H}_9\text{NH}_3)_2[\text{AlFZn}_2(\text{HPO}_3)_4]$	26	[3c]
	$\text{H}_2\text{tmdp} \cdot \text{Zn}_3(\text{HPO}_3)_4$	16	[3d]
SU-61	$(\text{Ge}, \text{Si})_{10}(\text{O}, \text{OH})_{28}$	26	[3e]
VSF-5	$\text{Ni}_{20}[(\text{OH})_{12}(\text{H}_2\text{O})_6][(\text{HPO}_4)_8(\text{PO}_4)_4] \cdot 12\text{H}_2\text{O}$	24	[3f]
ASU-16	$(\text{H}_2\text{dab})_3(\text{dab})_{10}[\text{Ge}_{14}\text{O}_{26}\text{F}_4] \cdot 16\text{H}_2\text{O}$	24	[3g]
FJ-1	$[\text{Ni}@\text{Ge}_{14}\text{O}_{24}(\text{OH})_3]$	24	[3h]
ZnHPO-CJ1	$[(\text{C}_4\text{H}_{12}\text{N})_2][\text{Zn}_3(\text{HPO}_3)_4]$	24	[3i]
NTHU-1	$[\text{Ga}_2(\text{DETA})(\text{PO}_4)_2] \cdot 2\text{H}_2\text{O}$	24	[3j]
SU-M	$[(\text{H}_2\text{MPMD})_2(\text{H}_2\text{O})_3][\text{Ge}_{10}\text{O}_{20.5}(\text{OH})_3]$	30	[3k]
BeHPO-1	$(\text{C}_2\text{H}_8\text{N})_2[\text{Be}(\text{HPO}_3)_4]$	16	[3l]
	$\text{EV} \cdot \text{Be}_2(\text{HPO}_4)_2(\text{H}_2\text{PO}_4)_2$	24	[3m]

induce the formation of 2D organic templated lanthanide sulfates. A 3D organic templated lanthanide sulfates with intersecting extra-large 20-membered ring channels, formulated as $[(\text{CH}_3)_2\text{NH}_2]_9[\text{Pr}_5(\text{SO}_4)_{12}] \cdot 2\text{H}_2\text{O}$ (**1**) and two novel 2D lanthanide sulfates with double-stranded chains, formulated as $[\text{H}_3\text{O}]_3[(\text{CH}_3)_2\text{NH}_2]_3[\text{Ln}_2(\text{SO}_4)_6]$ (Ln=Pr for **2**, Nd for **3**) were successfully synthesized.

1 Experimental

1.1 Materials and methods

The entire three compounds were prepared from a mixture of lanthanide oxide (99.9%), concentrated sulfuric acid (98%, *w/w*), *N,N*-dimethylformamide (DMF, 99.5%), and 1, 3, 5-triazine-2, 4, 6-triamine (99.7%) under solvothermal conditions. All chemicals purchased with reagent grade were used without further purification. The element analyses were performed on a Perkin-Elmer 2400 element analyzer and the inductively coupled plasma (ICP) analysis was performed on a Perkin-Elmer optima 3300 DV ICP spectrometer. The infrared (IR) spectra were recorded within the 400~4 000 cm^{-1} region on a Nicolet Impact 410 FTIR spectrometer using KBr pellets. A NETZSCH STA 449C unit was applied to carry out the TGA analyses under nitrogen atmosphere with a heating rate of 10 $^\circ\text{C} \cdot \text{min}^{-1}$.

1.2 Syntheses of compounds 1~2

$[(\text{CH}_3)_2\text{NH}_2]_9[\text{Pr}_5(\text{SO}_4)_{12}] \cdot 2\text{H}_2\text{O}$ (**1**): a solution was prepared by dissolving Pr_2O_3 (0.104 0 g, 0.315 3 mmol) into DMF (7.021 4 g, 0.096 mol) and sulfuric acid (1.525 8 g, 0.015 6 mol) under constant stirring for an hour. The resulting mixture was transferred into a 25 mL Teflon-lined stainless-steel autoclave and heated at 433 K for 6 days. After cooling to the room temperature, the product was washed with ethanol and dried in air for one day. Finally, the green block crystals (Yield: 61% based on Pr) were obtained. Elemental analysis Calcd. for $\text{C}_{18}\text{H}_{76}\text{Pr}_5\text{N}_9\text{O}_{50}\text{S}_{12}$ (%): C, 9.36; H, 3.29; N, 5.46. Found (%): C, 9.27; H, 3.28; N, 5.41. IR data (KBr pellet, cm^{-1}): 3 447 (b), 2 783 (w), 1 628 (m), 1 468 (m), 1 139 (b), 983 (m), 653 (m), 595 (m).

$[\text{H}_3\text{O}]_3[(\text{CH}_3)_2\text{NH}_2]_3[\text{Pr}_2(\text{SO}_4)_6]$ (**2**): The 2D green

block crystal of compound **2** was prepared in the same way. Pr_2O_3 (0.103 3 g, 0.313 2 mmol) was dissolved into DMF (7.260 3 g, 0.099 3 mol) and sulfuric acid (1.505 8 g, 0.015 4 mol) under constant stirring for an hour. Then 1, 3, 5-triazine-2, 4, 6-triamine (0.119 6 g, 0.948 3 mmol) was added into the solution under constant stirring for 30 minutes. The resulting mixture was transferred into a 25 mL Teflon-lined stainless-steel autoclave and heated at 433 K for 6 days. After cooling to the room temperature, the product was washed with ethanol and dried in air for one day to give the block crystals (Yield: 21% based on Pr). Elemental analysis Calcd. for $\text{C}_6\text{H}_{33}\text{Pr}_2\text{N}_3\text{O}_{27}\text{S}_6$ (%): C, 6.83; H, 3.13; N, 3.99. Found (%): C, 6.75; H, 3.17; N, 4.02. IR data (KBr pellet, cm^{-1}): 3 434 (b), 3 135 (b), 1 628 (m), 1 466 (w), 1 400 (m), 1 121 (m), 658 (m), 599 (m).

$[\text{H}_3\text{O}]_3[(\text{CH}_3)_2\text{NH}_2]_3[\text{Nd}_2(\text{SO}_4)_6]$ (**3**): The green block crystals of compound **3** was prepared in the same way by using Nd_2O_3 (0.102 3 g), instead of Pr_2O_3 (Yield: 39% based on Nd). Elemental analysis Calcd. for $\text{C}_6\text{H}_{33}\text{Nd}_2\text{N}_3\text{O}_{27}\text{S}_6$ (%): C, 6.79; H, 3.11; N, 3.96. Found (%): C, 6.67; H, 3.02; N, 3.99. IR data (KBr pellet, cm^{-1}): 3 433 (b), 3 134 (b), 1 628 (m), 1 465 (w), 1 400 (m), 1 122 (m), 652 (m), 594 (m).

1.3 X-ray crystallography

The single crystals (0.14 mm×0.13 mm×0.12 mm for **1**, 0.12 mm×0.12 mm×0.09 mm for **2**, 0.13 mm×0.12 mm×0.11 mm for **3**) of the title compounds were chosen onto a thin glass fiber by epoxy glue in air for data collection. And the diffraction data were collected on a Bruker Smart Apex 2 CCD with Mo $K\alpha$ radiation ($\lambda=0.071\ 073\ \text{nm}$) at 296(2) K using φ - ω scan method. An empirical absorption correction was performed on SADABS program^[13]. All the non-hydrogen atoms were refined anisotropically, while the hydrogen atoms of organic molecule were refined in calculated positions, assigned isotropic thermal parameters, and allowed to ride on their parent atoms. The structures were solved by direct methods using the SHELXS-2014 program and refined with full-matrix least squares on F^2 using the SHELXL-2014/7 program^[14]. Further details of the X-ray structural

Table 2 Crystal data and structure refinement for compounds 1~3

Compound	1	2	3
Empirical formula	C ₁₈ H ₇₆ Pr ₅ N ₉ O ₅₀ S ₁₂	C ₆ H ₃₃ Pr ₂ N ₃ O ₂₇ S ₆	C ₆ H ₃₃ Nd ₂ N ₃ O ₂₇ S ₆
Formula weight	2 308.27	1 053.59	1 060.25
Crystal system	Monoclinic	Triclinic	Triclinic
Space group	<i>C2/c</i>	<i>P</i> $\bar{1}$	<i>P</i> $\bar{1}$
<i>a</i> / nm	2.067 15(18)	1.010 92(16)	1.009 3(2)
<i>b</i> / nm	3.608 5(3)	1.255 8(2)	1.253 0(3)
<i>c</i> / nm	1.015 40(9)	1.376 2(2)	1.370 6(3)
α / (°)		68.815(2)	68.713(2)
β / (°)	114.677 0(10)	69.951(2)	69.882(2)
γ / (°)		79.100(2)	78.831(2)
<i>V</i> / nm ³	6.882 5(11)	1.526 1(4)	1.511 9(6)
<i>Z</i>	4	2	2
<i>D_c</i> / (Mg·m ⁻³)	2.228	2.293	2.329
Absorption coefficient / mm ⁻¹	3.949	3.672	3.918
<i>F</i> (000)	4 536	1 040	1 044
θ range for data collection / (°)	1.13~25.25	1.66~25.50	1.67~25.50
Limiting indices	-22 ≤ <i>h</i> ≤ 24, -38 ≤ <i>k</i> ≤ 43, -12 ≤ <i>l</i> ≤ 11	-12 ≤ <i>h</i> ≤ 12, -15 ≤ <i>k</i> ≤ 15, -15 ≤ <i>l</i> ≤ 16	-11 ≤ <i>h</i> ≤ 12, -15 ≤ <i>k</i> ≤ 15, -16 ≤ <i>l</i> ≤ 16
Reflections collected, unique	19 062, 6 224 (<i>R</i> _{int} =0.035 1)	11 088, 5 567 (<i>R</i> _{int} =0.026 8)	10 822, 5 484 (<i>R</i> _{int} =0.036 1)
Completeness / %	99.70	97.90	97.50
Max. and min. transmission	0.648 7 and 0.607 9	0.733 5 and 0.667 0	0.672 5 and 0.629 9
Data, restraint, parameter	6 224, 36, 431	5 567, 66, 436	5 484, 67, 436
Goodness-of-fit on <i>F</i> ²	1.109	1.191	1.143
Final <i>R</i> indices ^{ab} [<i>I</i> > 2σ(<i>I</i>)]	<i>R</i> ₁ =0.033 4, <i>wR</i> ₂ =0.087 7	<i>R</i> ₁ =0.038 9, <i>wR</i> ₂ =0.109 3	<i>R</i> ₁ =0.044 4, <i>wR</i> ₂ =0.115 6
<i>R</i> indices ^{ab} (all data)	<i>R</i> ₁ =0.045 3, <i>wR</i> ₂ =0.103 1	<i>R</i> ₁ =0.050 9, <i>wR</i> ₂ =0.120 8	<i>R</i> ₁ =0.058 0, <i>wR</i> ₂ =0.127 0

$$^a R_1 = \sum ||F_o| - |F_c|| / \sum |F_o|; ^b wR_2 = \sum [w(F_o^2 - F_c^2)^2] / \sum [w(F_o^2)^2]^{1/2}.$$

analyses for compounds **1**~**3** are given in Table 2.

CCDC: 1553358, **1**; 1553359, **2**; 1553360, **3**.

2 Results and discussion

2.1 Synthesis

The solvothermal synthesis method has been demonstrated to be a useful technique in the formation of inorganic solid state materials. During the solvothermal synthesis, many factors including reaction temperature, pH values, solvent and time affect the nucleation and the crystal growth of the final products. In the formation of the title compound, the solvent (DMF) plays an important role. In the reaction, DMF decomposed into dimethylamine and formic acid. Solvothermal reaction of Pr₂O₃, DMF, and H₂SO₄ in a molar ratio of 1:680:110 were mixed to

produce a 3D structure with intersecting extra-large 20-membered ring (20MR) channels organic templated lanthanide sulfates, formula with [(CH₃)₂NH₂]₉[Pr₅(SO₄)₁₂]·2H₂O(**1**). Two dimensional inorganic lanthanide sulfates [H₃O]₃[(CH₃)₂NH₂]₃[Ln₂(SO₄)₆] (Ln=Pr for **2**, Nd for **3**) were obtained under similar conditions, except with the addition of second SDA into the stainless-steel autoclave. Therefore, large organic molecules (1,3,5-triazine-2,4,6-triamine) prevent the formation of 3D framework as a second template.

2.2 Description of the structure

2.2.1 Crystal structure of compound **1**

Compound **1** crystallizes in monoclinic space group *C2/c*. Crystal structural analysis indicates that the open framework of **1** is a porous praseodymium sulfate with extra-large 20MR channels. The open

framework of **1** is constructed from $[\text{PrO}_x]$ and $[\text{SO}_4]$ polyhedra to form a 3D inorganic anionic $\{\text{Pr}_5(\text{SO}_4)_{12}\}_n^{9-}$, with charge compensated by protonated dimethylamine cations.

The asymmetric unit of **1** contains two and a half praseodymium atoms, six sulfate groups, five protonated dimethylamine molecules and one free water molecule (Fig.1). In the inorganic open framework of **1**, Pr(1) and Pr(2) are eight-coordinated by O atoms from six sulfates ions, forming distorted bicapped trigonal prism geometry; Pr(3) is nine-coordinated by O atoms from six sulfates ions, forming distorted tricapped trigonal prism geometry. The average bond distances of Pr-O is 0.249 6 nm, whereas the angles of O-Pr-O are between $54.37(9)^\circ$ and $165.68(11)^\circ$. Six crystallographic independent S atoms can be divided into 4 groups: S(1) and S(4) are bonded by one μ_3 -O atom, two μ_2 -O atoms and one O atom to make 4 S-O-Pr linkages; S(2) and S(5) are bonded by four μ_2 -O atoms to make 4 S-O-Pr linkages, S(3) is coordinated

by three μ_2 -O atoms and one O atom to make three S-O-Pr linkages; S(6) is bonded by two μ_2 -O atoms and two O atoms to make two S-O-Pr linkages. All the S atoms are tetrahedrally coordinated by four O atoms with the S-O distances 0.138 9(5) to 0.151 4(3) nm, comparable to those of similar bonds reported earlier^[7-8].

The structure of **1** can be described as constructed from two types of secondary building units (SBUs). Two $\{\text{Pr}_3(\text{SO}_4)_6\}^{3-}$ fragments connect each other by sharing Pr(1) to make the SBU-1: $\{\text{Pr}_5(\text{SO}_4)_{12}\}^{9-}$. Two adjacent SBU-1s are linked by bridging O atoms to generate an interesting 20-membered ring (Fig.2a). Two adjacent SBU-2s are linked by bridging O atoms to generate an interesting 10-membered ring (10MR, Fig.2b). Neighboring 10 and 20-membered rings are connected by bridging SO_4 groups to form an open framework with a 3D channel system (Fig.3a). Although both 10 and 20-membered channels keep a different size, they can be arranged in an ordered close packing arrangement just like mesoporous materials. Each 20MR channel is surrounding by six 10MRs, and these are alternately surrounded by three 20MRs and three 10MRs channels. The approximate window sizes for 20MR and 10MR are $0.53 \text{ nm} \times 0.94 \text{ nm}$ and $0.38 \text{ nm} \times 0.38 \text{ nm}$, respectively. Interestingly, there are other rectangular 20MR channels along the crystallographic $[101]$ direction (Fig.3b), which pore size is $0.28 \text{ nm} \times 1.28 \text{ nm}$. We used the PLATON software to calculate the percent void volume in the 3D network of **1**, and the result is 48.9%. This is similar with our previous work^[8d,12].

As shown in Fig.4, the protonated dimethylamine molecules and free water molecules are located in the 10MR and both types of 20MR channels of the inorganic framework by using the strong hydrogen bonding interactions between H atoms of organic amine molecules and O atoms of the open-framework of **1**. The free water molecules in 20MR channels are connected each other by strong hydrogen bonding to form a zigzag chain along c axis, since the bond between two adjacent water molecules are 0.281 2 and 0.291 0 nm (Fig.4d).

2.2.2 Crystal structure of compounds **2** and **3**

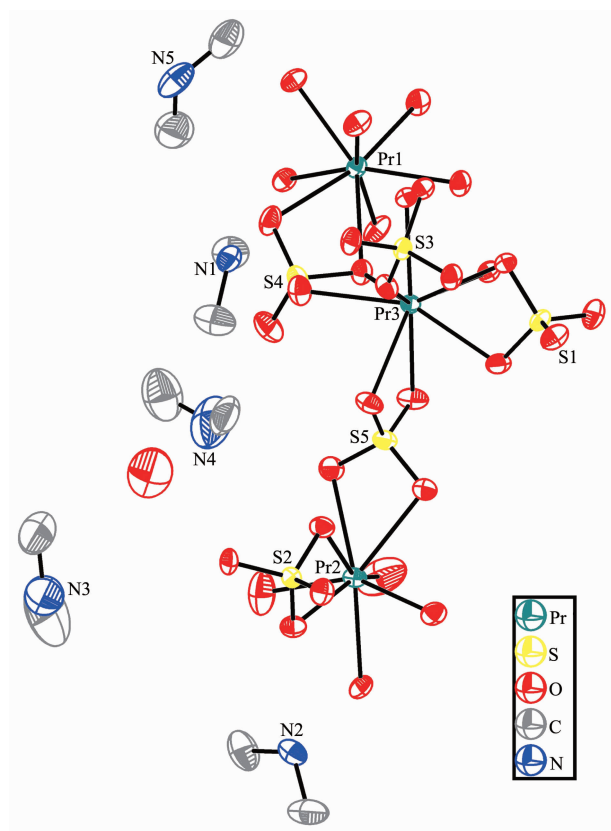


Fig.1 ORTEP view of the $[(\text{CH}_3)_2\text{NH}_2]_9[\text{Pr}_5(\text{SO}_4)_{12}] \cdot 2\text{H}_2\text{O}$ structure showing the atom labeling scheme with 50% probability

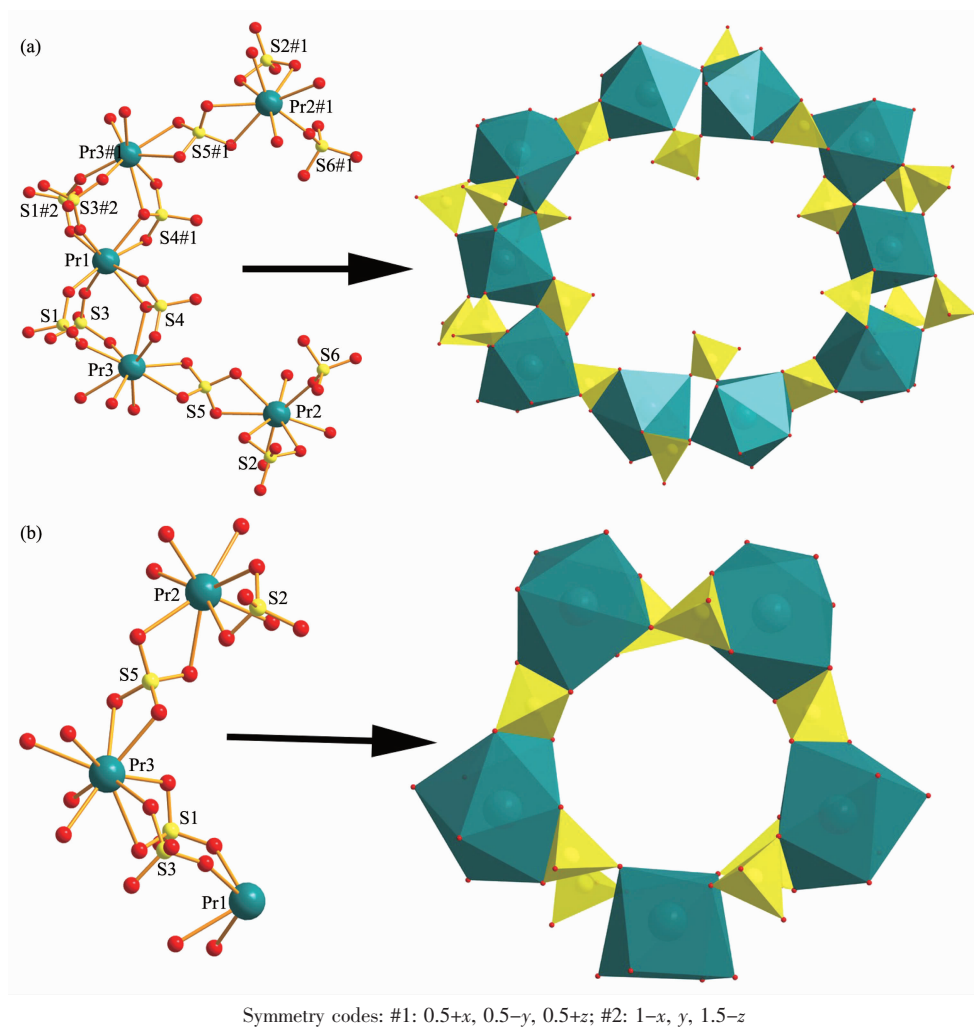


Fig.2 (a) Two adjacent SUB-1 connected by SO_4 tetrahedral to form a 20MR channel in **1**;
(b) Two adjacent SUB-2 connected by SO_4 tetrahedral and Pr1 to form a 10MR channel in **1**

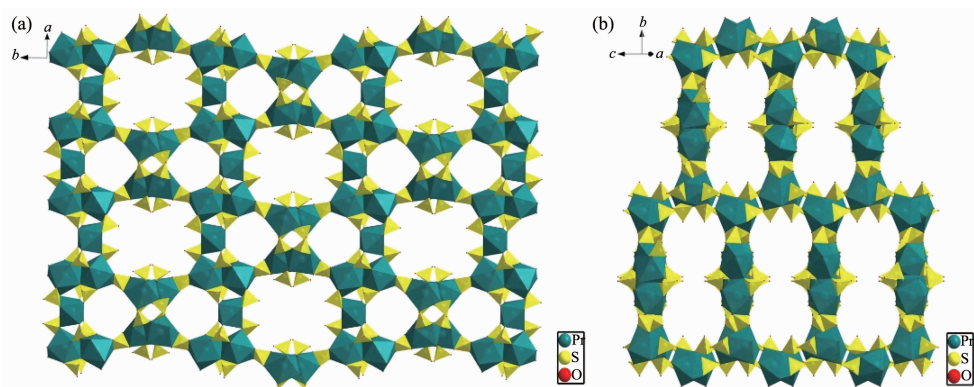


Fig.3 (a) Polyhedral representation of open framework including 10MR and 20MR channels of **1** along c axis;
(b) Rectangle 20MR-2 channels along the crystallographic $[101]$ direction

Compounds **2** and **3** are isostructural and crystallize in triclinic space group $P\bar{1}$. We take compound **2** as example to describe the structure. The structure of **2** consists of a 2D inorganic anionic

$\{\text{Pr}_2(\text{SO}_4)_6\}_n^{6n-}$ layer, charge compensated by the protonated dimethylamine molecules and hydrated protons. The asymmetric unit of **2** contains two praseodymium atoms, six sulfate groups, three protonated

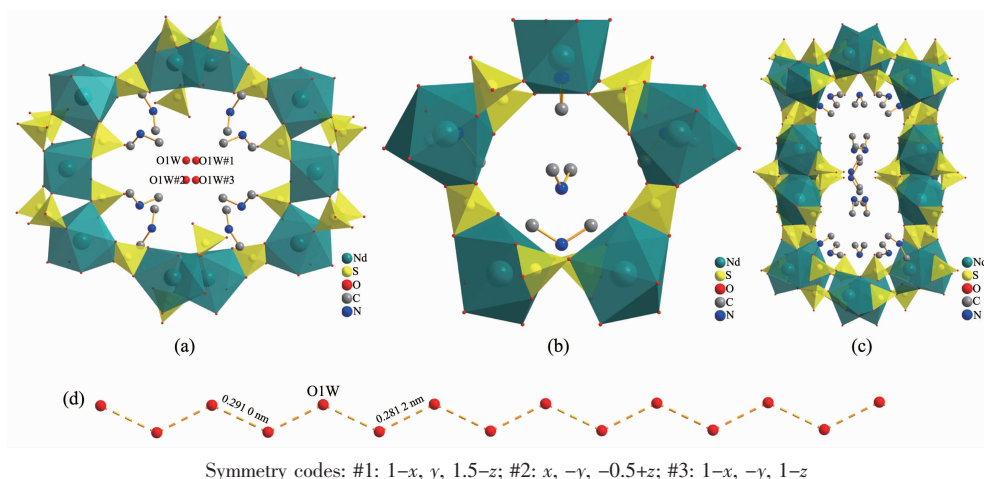


Fig.4 (a) Protonated dimethylamine molecules and water molecules located in the 20MR-1; (b, c) Protonated dimethylamine molecules in the 10MR and 20MR-2; (d) Zigzag chain of water molecules by strong hydrogen bond in the 20MR-1 channels

dimethylamine molecules and three hydrated protons (Fig.5). In the inorganic layer of **2**, Pr(1) is nine-coordinated by O atoms from six sulfates, forming distorted tricapped trigonal prismatic geometry; Pr(2) is eight-coordinated by eight O atoms from six sulfates, forming distorted bicapped trigonal prismatic geometry. The average bond distances of Pr-O is 0.251 4 nm, whereas the angles of O-Pr-O are between 52.34(12)° and 157.18(13)°. Of the six crystallographic independent S atoms, S(1) and S(2) form 2 S-O-Pr linkages through two μ_2 -O atoms; S(3), S(5) and S(6) make 3 S-O-Nd linkages through three μ_2 -O atoms; S(4) forms 4

S-O-Pr linkages through four μ_2 -O atoms. All the S atoms are tetrahedrally coordinated by four O atoms with the S-O distances of 0.143 4(6) to 0.151 3(4) nm, comparable to those of similar bonds reported earlier^[7-8].

The framework structure of **2** is made from the tetrahedral (polyhedral) linkage between $[\text{PrO}_x]$ and $[\text{SO}_4]$ moieties sharing vertexes or edges. The connectivity between these units forms anionic layers, which are anionic. The protonated SDA (dimethylamine) and protonated water (H_3O^+) cations are occupied spaces between the layers to compensate the charge. To the best of our knowledge, protonated water (H_3O^+) cation was barely observed in the previously reported organic templated lanthanide sulfates^[8,12]. The connectivity between the $[\text{PrO}_x]$ and $[\text{SO}_4]$ units produces two distinct types of chains, labeled chain A and B. The A type chain is a double-stranded chain that consists of four-membered rings involving Pr(1), Pr(2), S(4) and S(6), while the B type chain is made up of eight-membered rings (Fig.6). These kinds of double-stranded chains are particularly rare in inorganic materials, because only one sulfate, one phosphate and one arsenate were reported, formulated as $[\text{H}_3\text{N}(\text{CH}_2)_2\text{NH}_3][\text{FeF}_3(\text{SO}_4)]$ ^[11a], $[\text{NH}_3(\text{CH}_2)_2\text{NH}(\text{CH}_2)_2\text{NH}_3][\text{Zn}_2\text{PO}_4(\text{HPO}_4)]_2$ ^[11b] and $[\text{C}_4\text{N}_2\text{H}_{12}][\text{Fe}(\text{OH})(\text{HAsO}_4)(\text{C}_2\text{O}_4)] \cdot \text{H}_2\text{O}$ ^[11c]. The chains are connected to one another, forming a layer (Fig.7). It is some kinds of interests that there are two kinds of eight-membered

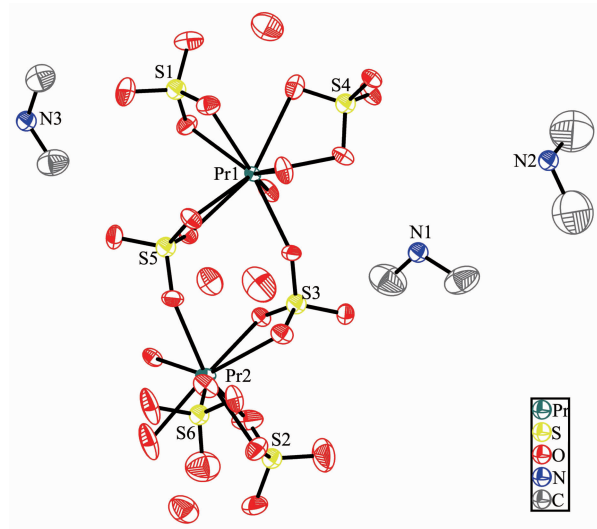


Fig.5 ORTEP view of the $[\text{H}_3\text{O}]_3[(\text{CH}_3)_2\text{NH}_2]_3[\text{Pr}_2(\text{SO}_4)_6]$ structure showing the atom labeling scheme with 50% probability

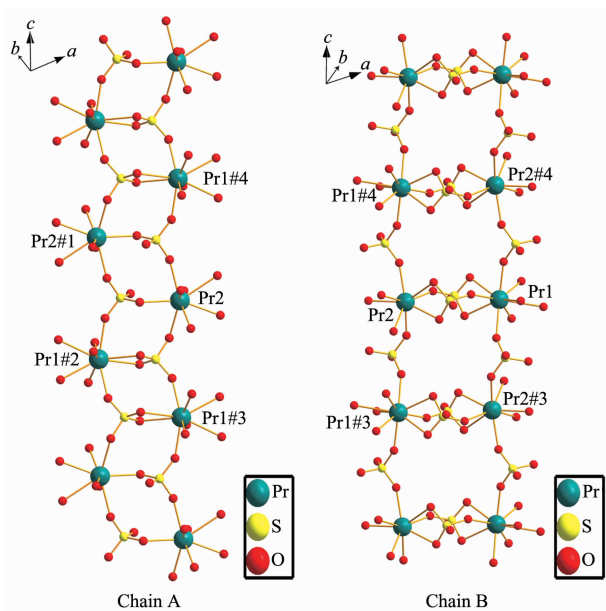


Fig.6 View of different types of chain arrangements in $[\text{H}_3\text{O}]_3[(\text{CH}_3)_2\text{NH}_2]_3[\text{Pr}_2(\text{SO}_4)_6]$

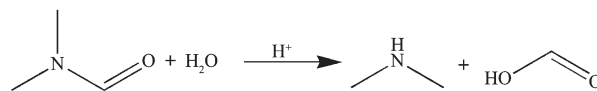
rings in chain B, one is consisting of $[-\text{Pr}1-\text{S}6-\text{Pr}2-\text{S}3-\text{Pr}1-\text{S}6-\text{Pr}2-\text{S}3-\text{Pr}1-]$, which dimension is $0.563 \text{ nm} \times 0.683 \text{ nm}$; the other is consisting of $[-\text{Pr}2-\text{S}4-\text{Pr}1-\text{S}3-\text{Pr}2-\text{S}4-\text{Pr}1-\text{S}3-\text{Pr}2-]$, which dimension is $0.548 \text{ nm} \times 0.627 \text{ nm}$ (Fig.7). To the best of our knowledge, this lanthanide sulfate is the first example of an open framework material where different types of chain arrangements are connected to each other forming a

layer.

As we know, only two previously reported organic templated lanthanide sulfates contain protonated water (H_3O^+) cation^[8b,12]. Interestingly, this is a new example contains hydrated proton (H_3O^+). O3W makes four hydrogen bonds $\text{O}-\text{H} \cdots \text{O}$ with the O atoms from double layers to generate 3D soft open framework along a axis (Fig.8a and b). The protonated dimethylamine cations and the remaining hydrated protons are located in the channels and involved hydrogen bonding interactions with the soft framework and make it more stable (Fig.8c).

2.3 Discussion

It is somewhat curious that compounds **2** and **3** include fully protonated dimethylamine instead of 1,3,5-triazine-2,4,6-triamine. Dimethylamine, along with formic acid, would be the product of decomposition of DMF as shown in Scheme 1^[15]. In the synthesis of compound **1**, DMF is employed as solvent as well as the organic template to form 3D mesoporous material. When we adding a big organic amine 1,3,5-triazine-2,4,6-triamine during the synthesis process, the products were 2D layered compounds (**2** and **3**).



Scheme 1

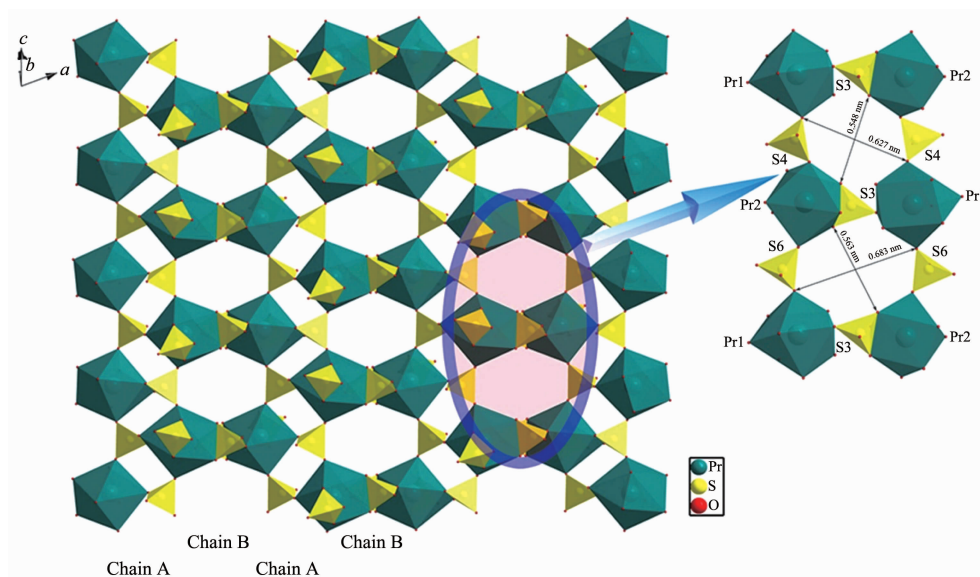


Fig.7 Polyhedral view of inorganic framework in **2** and the size of two kinds of 8-membered rings

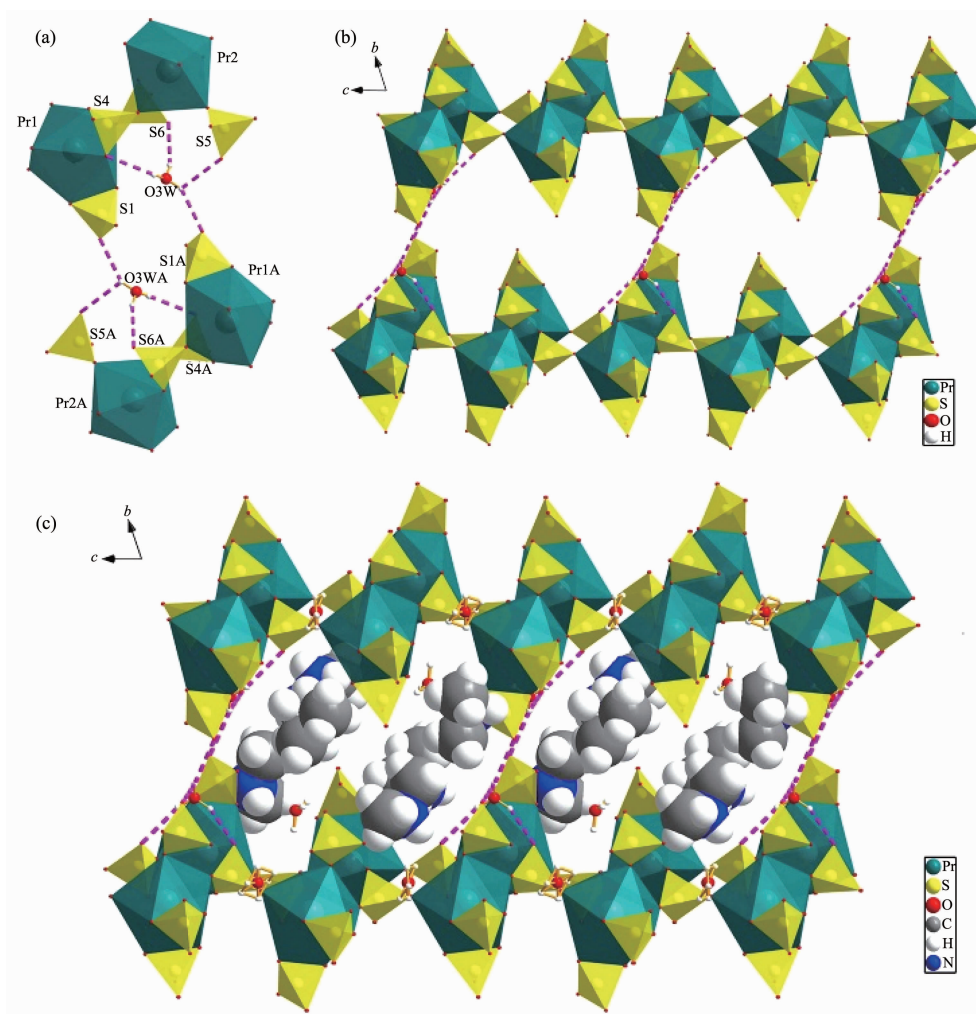


Fig.8 (a) Hydrogen bonding scheme of the O3w cation; (b) O3w cation connecting adjacent layers by four hydrogen bonds to make 3D soft open framework along *a* axis; (c) Guest cations (fully protonated organic amine molecules and the remaining hydrated protons) located in the channels

We thought that the second SDA (1,3,5-triazine-2,4,6-triamine) would be a cutting machine induces the formation of 2D layered compounds.

2.4 IR spectra

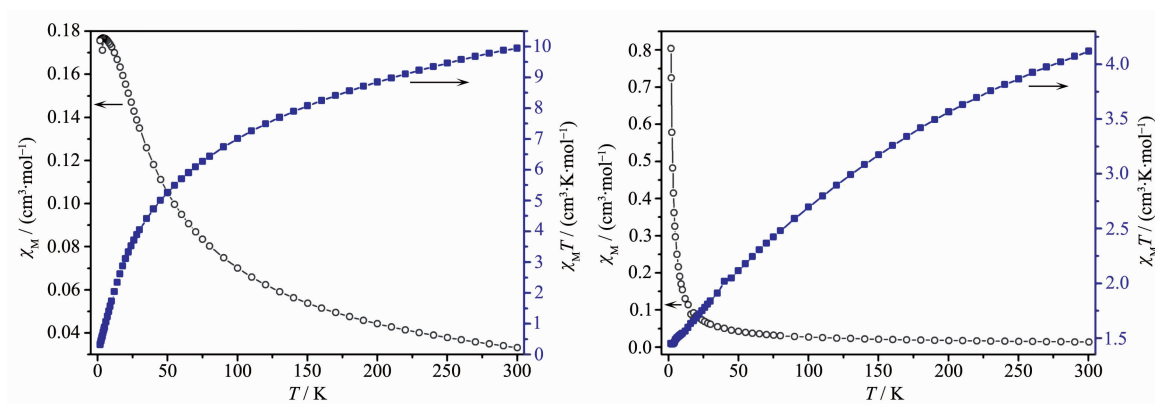
The IR spectra of compound **1** shows the characteristic bands for dimethylamine in the region of 1 400~1 600 cm^{-1} . The strong bands around 1 140 cm^{-1} can be attributed to the sulfate ion. Absorption at 595 cm^{-1} is due to Pr-O vibration. A band around 3 440 cm^{-1} can be attributed to the presence of water.

The IR spectra of compounds **2** and **3** show the characteristic bands for dimethylamine in the region of 1 400~1 600 cm^{-1} . The strong bands around 1 120 cm^{-1} can be attributed to the sulfate ion. Absorption at 594 cm^{-1} is due to Pr-O vibration. A band around

3 390 cm^{-1} can be attributed to the presence of water.

2.5 Magnetic property

The variable-temperature magnetic susceptibility for compounds **1** and **3** were performed to investigate its preliminary magnetic studies in the range of 2~300 K under 100 Oe field. For compound **1** (Fig.9a), the $\chi_M T$ value is 9.95 $\text{cm}^3 \cdot \text{K} \cdot \text{mol}^{-1}$ at room temperature, which is larger than the calculated value (8.00 $\text{cm}^3 \cdot \text{K} \cdot \text{mol}^{-1}$) of five uncoupled ($S=1$) spins of Pr(III) atoms. Upon cooling, the value of $\chi_M T$ decreases continuously and reaches 0.32 $\text{cm}^3 \cdot \text{K} \cdot \text{mol}^{-1}$ at 2 K, resulting from the occurrence of intermolecular antiferromagnetic interaction among neighbor Pr(III) ions. The magnetic data of **1** were fitted to the Curie-Weiss law in the range of 100~300 K, and the best fit was $C=12.678$

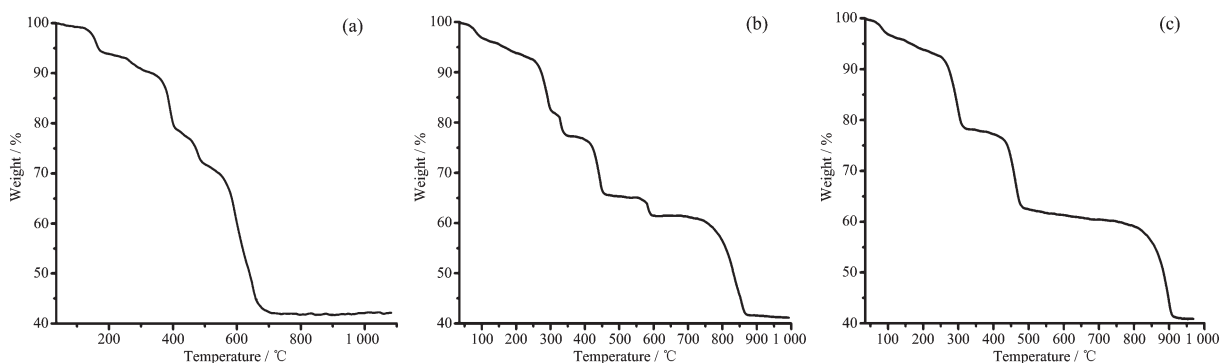
Fig.9 Temperature dependence of $\chi_M T$ and χ_M for **1** (a) and **3** (b)

$\text{cm}^3 \cdot \text{K} \cdot \text{mol}^{-1}$ and $\theta = -84.65$ K, characteristic of the antiferromagnetic interactions of **1**. For compound **3** (Fig.9b), the $\chi_M T$ value is $4.12 \text{ cm}^3 \cdot \text{K} \cdot \text{mol}^{-1}$ at room temperature, which is larger than the calculated value ($3.28 \text{ cm}^3 \cdot \text{K} \cdot \text{mol}^{-1}$) of two uncoupled ($S=3/2$) spins of Nd(III) atoms. Upon cooling, the value of $\chi_M T$ decreases continuously and reaches $1.45 \text{ cm}^3 \cdot \text{K} \cdot \text{mol}^{-1}$ at 2 K, resulting from the occurrence of intermolecular antiferromagnetic interaction among neighbor Nd(III) ions. The magnetic data of **3** were fitted to the Curie-Weiss law in the range of 110~300 K, and the best fit was $C=5.732 \text{ cm}^3 \cdot \text{K} \cdot \text{mol}^{-1}$ and $\theta=-120.18$ K, characteristic of the antiferromagnetic interactions of **3**.

2.6 Thermal behavior

The thermogravimetric analyses (TGA) of compounds **1**~**3** were performed in a N_2 atmosphere when heated to $1\,000\text{ }^\circ\text{C}$ at a rate of $10\text{ }^\circ\text{C} \cdot \text{min}^{-1}$. For compound **1**, the total weight loss is 59.6%, which is in agreement with the calculated value 62.3% (Fig. 10a). The weight loss of 6.4% in the range of 30~220 $^\circ\text{C}$ corresponds to the removal of two free water

molecules and some of dimethylamine. The second step loss of 25.5% in the range of 220~550 $^\circ\text{C}$ can be attributed to all the dimethylamine and some of SO_3 . The weight loss of 27.7% in the range of 550~1 080 $^\circ\text{C}$ can be attributed to the loss of SO_3 . The final product is Pr_2O_3 . For compound **2**, the total weight loss is 58.9%, which is in agreement with the calculated value 64.1% (Fig.10b). The weight loss of 7.3% in the range of 30~220 $^\circ\text{C}$ corresponds to the removal of three free water molecules. The second step loss of 17.8% in the range of 220~400 $^\circ\text{C}$ can be attributed to the decomposition of all the dimethylamine molecules. The weight loss of 33.8% in the range of 400~800 $^\circ\text{C}$ can be attributed to the loss of SO_3 . The final product is Pr_2O_3 . For compound **3**, the total weight loss is 59.4%, which is in agreement with the calculated value 63.6% (Fig.10c). The weight loss of 6.1% in the range of 30~200 $^\circ\text{C}$ corresponds to the removal of three free water molecules. The second step loss of 16.2% in the range of 200~380 $^\circ\text{C}$ can be attributed to the decomposition of all the

Fig.10 TG curves for compounds **1** (a), **2** (b) and **3** (c)

dimethylamine molecules. The last-step loss of 43.2% in the range of 380~980 °C can be attributed to the loss of all the SO₃. The final product is Nd₂O₃.

3 Conclusions

In summary, we have successfully synthesized three lanthanide sulfates by using DMF as solvent. DMF is decomposed into dimethylamine and formic acid, and the dimethylamine acts as an organic template. The 1,3,5-triazine-2,4,6-triamine as a second SDA is essential to the formation of 2D layer. The 2D layered compounds **2** and **3** are constructed by two different chains. Without second SDA, the product appears to be 3D mesoporous material of compound **1**. The syntheses of the compounds demonstrated that the solvent, lanthanide elements and 1,3,5-triazine-2,4,6-triamine play a vitally important role, and lanthanide sulfates can be designed and prepared by applying solvothermal method.

References:

- [1] (a) Cheetham A K, Ferey G, Loiseau T. *Angew. Chem. Int. Ed.*, **1999**, **38**(22):3268-3292
(b) Thomas J M, Raja R, Sankar G, et al. *Acc. Chem. Res.*, **2001**, **34**(3):191-200
(c) Yu J, Xu R. *Acc. Chem. Res.*, **2003**, **36**(7):481-490
(d) Natarajan S, Mandal S. *Angew. Chem., Int. Ed.*, **2008**, **47**(26):4798-4828
(e) Jiang J, Yu J, Corma A. *Angew. Chem. Int. Ed.*, **2010**, **49**(18):3120-3145
(f) Xing H Z, Yang W T, Su T, et al. *Angew. Chem. Int. Ed.*, **2010**, **49**(13):2328-2331
(g) Shi M J, Lin C H, Wang S L. *J. Am. Chem. Soc.*, **2016**, **138**(21):6719-6722
- [2] Davis M E, Saldarriaga C, Montes C, et al. *Nature*, **1988**, **331**(6158):698-699
- [3] (a) Zhu J, Bu X, Feng P, et al. *J. Am. Chem. Soc.*, **2000**, **122**(46):11563-11564
(b) Li J, Li L, Liang J, et al. *Cryst. Growth Des.*, **2008**, **8**(7):2318-2323
(c) Lai Y L, Lii K H, Wang S L. *J. Am. Chem. Soc.*, **2007**, **129**(17):5350-5351
(d) Lin Z, Nayek H P, Dehnen S. *Inorg. Chem.*, **2009**, **48**(8):3517-3519
(e) Christensen K E, Bonneau C, Gustafsson M, et al. *J. Am. Chem. Soc.*, **2008**, **130**(12):3758-3759
(f) Guillou N, Gao Q, Forster P M, et al. *Angew. Chem., Int. Ed.*, **2001**, **40**(15):2831-2834
(g) Plivert J, Gentz T M, Laine A, et al. *J. Am. Chem. Soc.*, **2001**, **123**(50):12706-12707
(h) Lin Z, Zhang J, Zhao J, et al. *Angew. Chem., Int. Ed.*, **2005**, **44**(42):6881-6884
(i) Liang J, Li J, Yu J, et al. *Angew. Chem., Int. Ed.*, **2006**, **45**(16):2546-2548
(j) Lin C H, Wang S L, Lii K H. *J. Am. Chem. Soc.*, **2001**, **123**(19):4649-4650
(k) Zou X, Conradsson T, Klingstedt M, et al. *Nature*, **2005**, **437**(7059):716-719
(l) Luo X C, Luo D D, Gong M C, et al. *CrystEngComm*, **2011**, **13**(11):3646-3648
(m) Wang K C, Li J, Xu D G, et al. *CrystEngComm*, **2015**, **17**(10):2162-2167
- [4] Rao C N R, Behera J N, Dan M. *Chem. Soc. Rev.*, **2006**, **35**(4):375-387
- [5] (a) Dan M, Behera J N, Rao C N R. *J. Mater. Chem.*, **2004**, **14**(8):1257-1265
(b) Doran M, Norquist A, O'Hare D. *Chem. Commun.*, **2002**(24):2946-2947
- [6] (a) Bataille T, Lotier D. *J. Solid State Chem.*, **2004**, **177**(4/5):1235-1243
(b) Bataille T, Lotier D. *J. Mater. Chem.*, **2002**, **12**(12):3487-3493
- [7] (a) Zhang Y, Huang L, Miao H, et al. *Chem. Eur. J.*, **2015**, **21**(8):3234-3241
(b) Lin Q F, Zhang Y, Cheng W W, et al. *Dalton Trans.*, **2017**, **46**(3):643-646
(c) Lin Q F, Li J, Dong Y Y, et al. *Dalton Trans.*, **2017**, **46**(30):9745-9749
(d) Liu Y, Zhang Y, Hu G H, et al. *Chem. Eur. J.*, **2015**, **21**(29):10391-10399
(e) Xu Y, Ding S H, Zheng X. *J. Solid State Chem.*, **2007**, **180**(7):2020-2025
(f) Zhu Y L, Zhou G P, Xu Y, et al. *Z. Anorg. Allg. Chem.*, **2008**, **634**(3):545-548
- [8] (a) Zhou W L, Chen Q, Zhu D R, et al. *Z. Anorg. Allg. Chem.*, **2009**, **635**(3):572-576
(b) Zhu Y L, Sun X C, Zhu D R, et al. *Inorg. Chim. Acta*, **2009**, **362**(8):2565-2568
(c) Zhou W L, Chen Q, Jiang N, et al. *Inorg. Chim. Acta*, **2009**, **362**(9):3299-3302
(d) Zheng L, Xu Y, Zhang X L, et al. *CrystEngComm*, **2010**, **12**(3):694-696

- (e)Zhou W L, Ding X R, Zhang Z B, et al. *Z. Anorg. Allg. Chem.*, **2009**,**636**(5):882-885
- (f)Zhou W L, Xu Y, Han L J, et al. *Dalton Trans.*, **2010**,**39**(15):3681-3686
- (g)Zheng L, Zhang Z B, Zhu D R, et al. *Inorg. Chem. Commun.*, **2011**,**14**(1):258-260
- (h)Zheng L, Qiu X M, Zhang Z B, et al. *Inorg. Chem. Commun.*, **2011**,**14**(6):906-909
- [9] (a)Jia D, Zhang Y, Dai J, et al. *Inorg. Chem. Commun.*, **2005**,**8**(7):588-591
- (b)Fu J, Zheng L, Yuan Y, et al. *J. Chem. Crystallogr.*, **2011**,**41**(11):1737-1741
- (c)Fu J, Zheng L, Zhang Z B, et al. *Inorg. Chim. Acta*, **2012**,**383**:112-117
- (d)Zhang D, Lu Y, Chen L, et al. *CrystEngComm*, **2012**,**14**(20):6627-6638
- (f)Zhang D, Lu Y, Zhu D R, et al. *Inorg. Chem.*, **2013**,**52**(6):3253-3258
- (g)Zhang D, Fan X R, Lu Y, et al. *Chem. Res. Chin. Univ.*, **2013**,**29**(1):10-14
- [10]Zhou Y, Zhu H, Chen Z, et al. *Angew. Chem. Int. Ed.*, **2001**,**40**(11):2166-2168
- [11](a)Paul G, Choudhury A, Rao C N R. *Chem. Mater.*, **2003**,**15**(5):1174-1180
- (b)Neeraj S, Natarajan S, Rao C N R. *Chem. Mater.*, **1999**,**11**(5):1390-1395
- (c)Chakrabarti S, Natarajan S. *Angew. Chem., Int. Ed.*, **2002**,**41**(7):1224-1226
- [12]Zheng L, Qiu X M, Xu Y, et al. *CrystEngComm*, **2011**,**13**(7):2714-2720
- [13]*SMART* and *SADABS*, Bruker AXS Inc., Madison, Wisconsin, USA, **1997**.
- [14]Sheldrick G M. *SHELX 2014/7: Program for Crystal Structure Refinement*, University of Göttingen, Germany, **2014**.
- [15]Burrows A D, Cassar K, Friend R M W, et al. *CrystEngComm*, **2005**,**7**(89):548-550